International Journal of Thermophysics, Vol. 6, No. 6, 1985

# Now-Newtonian Flow Between Concentric Cylinders and the Effects of Finite Compressibility[1]

J. C. Rainwater[2] and H. J. M. Hanley[2]

Previous studies of the flow of a model soft-sphere liquid between rotating vertical concentric cylinders have predicted an enhanced depression of the free surface at the inner cylinder and the necessity and importance of accounting for finite compressibility. In those studies the rheological properties of the liquids were taken directly from computer simulations, whereas in the present work the liquid properties are altered in a controlled manner and the fluid dynamics problems is again solved numerically and self-consistently with the original boundary conditions. Specific alterations include the removal of all non-Newtonian properties, the change in sign of a generalized viscosity to create a rod-climbing or Weissenberg effect, and the removal of shear dilatancy or increase in pressure with shear. Our conclusion is that nonzero compressibility needs to be taken into account only in the presence of shear dilatancy.

**KEY WORDS:** compressibility; concentric cylinder; non-Newtonian flow; rheological behavior; shear dilatancy; soft-sphere liquid; Weissenberg effect.

## 1. INTRODUCTION

Recently we have examined the problem of non-Newtonian flow between vertical, rotating concentric cylinders [1]. The procedure was somewhat different from the usual in that we approached the problem given the transport coefficients of the fluid, rather than inferring the coëfficients from the macroscopic behavior resulting from the flow. The fluid in question was the model soft-sphere inverse-twelve system whose properties are available from computer simulation, nonequilibrium molecular dynamics (NEMD) [2]. The assumptions invoked in our solution are discussed in detail in Ref. 1.

---

[1] Paper presented at the Ninth Symposium on Thermophysical Properties, June 24–27, 1985, Boulder, Colorado, U.S.A.

[2] Thermophysics Division, National Bureau of Standards, Boulder, Colorado 80303, U.S.A.



0195-928X/85/1100-0595$04.50/0 

It is well known that, when the outer cylinder is stationary, a Newtonian-liquid free surface exhibits a small depression at the inner cylinder [3], whereas for typical non-Newtonian liquids (such as polymer melts and polymer solutions), the free surface exhibits a Weissenberg effect or climbing of the inner cylinder [3, 4]. Our calculations for the soft-sphere fluid demonstrated behavior not predicted by previous theoretical treatments of this flow problem [5]. In particular, the model liquid exhibited an enhanced depression at the inner cylinder that was much larger in magnitude than the Newtonian depression under equivalent conditions. Additionally, we found that the finite compressibility of the liquid, neglected in previous analyses, needed to be included explicitly in order to make the solution self-consistent.

Using the numerical methods developed in Ref. 1, we examine in this paper the consequences of certain changes in the fluid properties, so that the causes of the enhanced depression and sensitivity to compressibility are isolated. Special cases considered here include the Newtonian liquid with finite compressibility, the reversal in sign of a "generalized viscosity" $\eta_0$, which permits a Weissenberg effect, and the non-Newtonian liquid in the absence of shear dilatancy (increase in pressure with shear) [6]. Our overall conclusion is that the sensitivity of the flow profile to finite compressibility is closely tied to the presence of shear dilatancy.

## 2. PARAMETERS OF THE FLOW PROBLEM

Following the notation of Joseph and Fosdick [5], we denote the inner cylinder radius by $a$, the outer cylinder radius by $b$, the angular velocity of the inner cylinder by $\Omega$, the ratio of angular velocities of the outer to inner cylinders by $\lambda$, the cylindrical coordinate system by $\{r, \theta, z\}$, the stream velocity by $\mathbf{u}(\mathbf{r})$, and the free-surface height profile by $h(r)$. The pressure tensor $\mathbf{P}(\mathbf{r})$ has components $P_{ij}$, where $i, j = r, \theta, z$.

Soft-sphere fluid simulations, however, have been performed in Cartesian coordinates $\{x, y, z\}$, with unit vectors $\hat{e}_x, \hat{e}_y, \hat{e}_z$, for the Couette flow $\mathbf{u}(\mathbf{r}) = \gamma y \hat{e}_x$, where $\gamma$ is the shear rate. The pressure tensor $\mathbf{P}(\mathbf{r})$ is usually discussed with respect to the soft-sphere fluid NEMD simulations [2] in terms of the following alternate variables:

$$p = \frac{1}{3}(P_{xx} + P_{yy} + P_{zz}) \tag{1}$$

$$\eta_+ = -P_{xy}/\gamma = -P_{yx}/\gamma \tag{2}$$

$$\eta_- = -\frac{1}{2}(P_{xx} - P_{yy})/\gamma \tag{3}$$

$$\eta_0 = -\frac{1}{2}\left[P_{zz} - \frac{1}{2}(P_{xx} + P_{yy})\right]\Big/\gamma \tag{4}$$

By symmetry, $P_{xz} = P_{zx} = P_{yz} = P_{zy} = 0$. The generalized pressure $p$ and generalized viscosities $\eta_i$ are functions of the temperature, density, and shear rate, although the temperature dependence is not required since the steady-state flow is assumed to be isothermal.

The 108 ($N$) particle soft-sphere fluid was studied at the state point $X = 0.7$, where $X = \rho/(\sqrt{2}\, T^{1/4})$ with $\rho = N/V$, the density, and $T$ the temperature. In this paper we work with reduced units; see Ref. 2. $T$ was set at 1/4 so $X \equiv \rho$, which is 7/8 of the freezing density. For these conditions the shear-rate dependences of the pressure and the shear viscosity, $\eta_+$, can be represented by the expressions

$$p = 2.375 + 0.355\,\gamma^{3/2} \tag{5}$$

$$\eta_+ = 1.012 - 0.365\,\gamma^{1/2} \tag{6}$$

and the density dependences are given in Ref. 1. The shear-rate dependences of $\eta_-$ and $\eta_0$ are given by an approximate fit to the molecular dynamics data:

$$\eta_- = 0.02381\,\gamma^{1/2}/(0.1789 + \gamma^{3/2}) \tag{7}$$

$$\eta_0 = 0.04205\,\gamma^{3/2}/(0.07794 + \gamma^{5/2}) \tag{8}$$

The density dependences are not known but the derivatives are inferred via a relaxation-time hypothesis [7] to be

$$\frac{\partial \ln \eta_-}{\partial \ln \rho} = \frac{\partial \ln \eta_0}{\partial \ln \rho} = 2\frac{\partial \ln \eta_+}{\partial \ln \rho} - \frac{\partial \ln p}{\partial \ln \rho} \tag{9}$$

In Ref. 1 we examined in some detail the particular case $a = 0.2$, $b = 2.0$, $\Omega = -0.3$, and $\lambda = 0$.

## 3. EQUATIONS OF MOTION

It is assumed, following Ref. 1, that the pressure tensor depends only on the shear rate, not on vorticity or higher velocity gradients, and that deviations from tangentially symmetric flow $[\mathbf{u}(\mathbf{r}) = u_\theta(r)\hat{e}_\theta]$ may be neglected. Under these assumptions, the results for planar shear flow may be applied directly to cylindrical shear flow, with $x$ associated with $\theta$ and $y$ with $r$. The equations of motion then may be compactly represented by the following set of coupled nonlinear algebraic and integral equations:

$$\gamma(r)=\frac{B}{r^2\eta_+[\gamma(r),\rho(r)]};\qquad B=\text{constant} \tag{10}$$

$$u_\theta(r)=\Omega r+r\int_a^r\frac{\gamma(r')}{r'}\,dr' \tag{11}$$

$$P_{rr}(r)=P_{rr}(a)+\int_a^r dr'\left\{\frac{\rho(r')[u_\theta(r')]^2}{r'}-\frac{2\gamma(r')\,\eta_-[\gamma(r'),\rho(r')]}{r'}\right\} \tag{12}$$

$$P_{zz}(r)=P_{rr}(r)-\gamma(r)\{2\eta_0[\gamma(r),\rho(r)]+\eta_-[\gamma(r),\rho(r)]\} \tag{13}$$

$$P_{zz}(r)=p[\gamma(r),\rho(r)]-\frac{4}{3}\gamma(r)\,\eta_0[\gamma(r),\rho(r)] \tag{14}$$

with the boundary condition

$$u_\theta(b)=\Omega b+b\int_a^b\frac{\gamma(r)}{r}\,dr=\Omega\lambda b \tag{15}$$

The position-dependent density is written as

$$\rho(r)=\bar\rho+\delta\rho(r) \tag{16}$$

where $\bar\rho$ is the average density, and it is assumed that the density dependences of $p$ and $\eta_i$ may be linearized about $\delta\rho$; note also that

$$\int_a^b r\,dr\,\delta\rho(r)=0 \tag{17}$$

The free-surface height profile is

$$h(r)=[P_{zz}(r)+C]/\rho g,\qquad C=\text{constant} \tag{18}$$

where $g$ is the acceleration of gravity, so that the determination of $P_{zz}(r)$ is essentially equivalent to the determination of $h(r)$.

In Ref. 1, an algorithm was described for the solution of Eqs. (10)–(17) by means of numerical integration, numerical root finding, and repeated iteration. Details of the method are not repeated here.

## 4. SPECIAL CASES

### 4.1. Incompressible Liquid

The limit of an incompressible liquid is defined to be $(\partial p/\partial \rho) \rightarrow \infty$. It is, in practice, further implied that $(\partial \eta_i/\partial \rho)$, $i = +, -, 0$ is finite. When $\delta\rho(r)$ is small we have the linearized equations

$$p[\gamma(r), \rho(r)] = p[\gamma(r), \bar{\rho}] + \left(\frac{\partial p}{\partial \rho}\right) \delta\rho(r) \tag{19}$$

$$\eta_i[\gamma(r), \rho(r)] = \eta_i[\gamma(r), \bar{\rho}] + \left(\frac{\partial \eta_i}{\partial \rho}\right) \delta\rho(r) \tag{20}$$

In the incompressible limit, $(\partial p/\partial \rho)$ goes to infinity and $\delta\rho(r)$ goes to zero in such a way that the product $(\partial p/\partial \rho)\,\delta\rho(r)$ is finite. However, in the same limit the product $(\partial \eta_i/\partial \rho)\,\delta\rho(r)$ vanishes. Therefore, a solution to Eqs. (10)–(15) may be obtained by replacing $\eta_i[\gamma(r), \rho(r)]$ with $\eta_i[\gamma(r), \bar{\rho}]$, i.e., by neglecting the density dependence of the generalized viscosities, in Eqs. (10), (12), and (13), and by choosing a function for the product $(\partial p/\partial \rho)\,\delta\rho(r)$ such that Eq. (14) is in conformity with Eq. (13).

Conventional rheological theory [3] assumes liquids to be incompressible. In this case, Eq. (14) in effect decouples from Eqs. (10)–(13), and therefore shear dilatancy, i.e., the fact that $(\partial p/\partial \gamma) > 0$, does not contribute to the solution of the flow problem. However, as is shown in Ref. 1, such a decoupling is not warranted for the soft-sphere liquid. The key parameter is not the absolute magnitude of $\partial p/\partial \rho$ but, rather, the ratio of $\partial \ln p/\partial \ln \rho$ to $\partial \ln \eta_i/\partial \ln \rho$. For the particular example considered in Ref. 1, $\partial \ln p/\partial \ln \rho \approx 3.4$, $\partial \ln \eta_+/\partial \ln \rho \approx 4.3$, and, by Eq. (9), $\partial \ln \eta_-/\partial \ln \rho = \partial \ln \eta_0/\partial \ln \rho \approx 5.2$.

### 4.2. Compressible Newtonian Liquid

By definition for a Newtonian liquid, the pressure $p$ and the viscosity $\eta_+$, which reduces to the ordinary Newtonian shear viscosity $\eta$, are independent of the shear rate, although they depend on the density; also, $\eta_- = \eta_0 = 0$. The solution of Eqs. (10)–(13) and (15) for the incompressible Newtonian liquid is elementary and well known:

$$\gamma(r) = \frac{2a^2b^2(\lambda - 1)\Omega}{r^2(b^2 - a^2)} \tag{21}$$

$$u_\theta(r) = \Omega r + \frac{(\lambda - 1)\, a^2b^2\Omega r}{b^2 - a^2}\left[\frac{1}{a^2} - \frac{1}{r^2}\right] \tag{22}$$

$$P_{zz}(r)=P_{rr}(r)=p(r) \tag{23}$$

$$\begin{aligned} p(r)-p(b)= -\rho \Big\{ & \frac{1}{2}\Omega^2\left[1+(\lambda-1)\frac{b^2}{b^2-a^2}\right]^2 (b^2-r^2) \\ & - 2\Omega^2(\lambda-1)\frac{a^2b^2}{b^2-a^2}\left[1+(\lambda-1)\frac{b^2}{b^2-a^2}\right]\ln\frac{b}{r} \\ & + \frac{1}{2}(\lambda-1)^2\Omega^2\left(\frac{a^2b^2}{b^2-a^2}\right)^2\left(\frac{1}{r^2}-\frac{1}{b^2}\right)\Big\} \end{aligned} \tag{24}$$

For $\lambda=0$, Eq. (24) together with Eq. (18) describes a depression of the free surface at $r=a$ and a nearly flat free-surface profile near $r=b$. It is interesting to note that the solution is independent of viscosity. For the choice of parameters listed below Eq. (9), $P_{zz}(a)-P_{zz}(b)=-1.167\times10^{-3}$, approximately 2% of the enhanced depression found for the soft-sphere fluid in Ref. 1 [where $P_{zz}(a)-P_{zz}(b)=-6.07\times10^{-2}$]. This is consistent with the observation that, for the same $\Omega$, the depth of depression for a Newtonian liquid is much smaller than the height of climbing of a typical non-Newtonian liquid [3].

When compressibility is included, the solution in principle is changed. Because of centrifugal effects the pressure and, hence, the density are smaller near $r=a$. The viscosity is therefore also smaller, and from Eq. (10), $\gamma$ is larger. If $\lambda=0$, $u_\theta$ changes from $\Omega a$ at $r=a$ to zero at $r=b$ more steeply, and the lowered centrifugal force makes $p(r)-p(b)$ slightly smaller in absolute value.

Joseph and Fosdick [5] have solved the equations of motion for both the Newtonian liquid and the Rivlin-Erickson non-Newtonian liquid in a power series in $\Omega$. Although this power series is inappropriate for a liquid with rheological properties that are nonanalytic in $\gamma$, e.g., Eqs. (5)–(8), it appears to be sensible for the Newtonian liquid, so that $\delta\rho(r)$ may be expanded in a power series.

$$\delta\rho(r)=\Omega^2\delta\rho^{(1)}(r)+\Omega^4\delta\rho^{(2)}(r)+\cdots \tag{25}$$

where

$$\delta\rho^{(1)}(r)=\lim_{\Omega\to0}[p(r)-p(b)]/\Omega^2\left(\frac{\partial p}{\partial\rho}\right)+c_\rho \tag{26}$$

and $c_\rho$ is a normalization constant needed to satisfy Eq. (17).

Equations (10) and (12) may then be linearized in $\delta\rho$ by means of Eqs. (19) and (20), and the solution through linear order in $\delta\rho$ may be solved analytically. The constant $B$ is altered by a correction $\delta B$, $O(\Omega^3)$, and the correction to the pressure profile is $O(\Omega^4)$. The calculation is tedious but straightforward and involves only elementary integrations over products of powers and logarithms of $r$. However, the final explicit solutions are extremely lengthy and cumbersome, and consequently we quote numerical magnitudes for the analytic $O(\Omega^4)$ correction to $p(a) - p(b)$, in effect the depth of depression, only for two specific examples.

The dimensionless expansion parameter that characterizes the solution is $(\partial \ln \eta/\partial \ln \rho)(\partial \ln p/\partial \ln \rho)^{-1} \rho a^2\Omega^2/p$, which obviously vanishes in the incompressible limit. For the parameters listed below Eq. (9) and the zero shear-rate pressures and viscosities in Ref. 1 at $\rho = 0.7$ ($p = 2.375$, $\partial p/\partial\rho = 11.364$, $\eta = 1.012$ and $\partial\eta/\partial\rho = 7.019$), the change in $\Delta p = p(a) - p(b)$ is only $3.67 \times 10^{-7}$. Our numerical algorithms cannot confirm this result, since finite error limits must necessarily be set in the numerical integration and root finding subroutines, and the two solutions for $p(r)$ can be made to converge only within a finite tolerance, typically between $10^{-4}$ and $10^{-5}$.

If we set $\Omega = 2.0$, then in the incompressible limit $\Delta p = -5.19 \times 10^{-2}$, comparable to the non-Newtonian solution in Ref. 1. The $O(\Omega^4)$ change in $\Delta p$ from the analytic solution is $7.25 \times 10^{-4}$. From our numerical algorithm, the two solutions for $\Delta p$ converge to within a difference of $7.6 \times 10^{-5}$. Based on their average, the correction in $\Delta p$ due to finite compressibility is $9.12 \times 10^{-4}$, so that the analytic correction is 20% smaller. However, the expansion parameter here has a value of 0.064, and from higher-order terms, the percentage difference is linear in this parameter, so the agreement appears to be reasonable. The important point to note is that, even with a much larger rotation rate and a comparable depth of depression, the corrections due to finite compressibility for the Newtonian liquid are still an order of magnitude lower than those for the non-Newtonian liquid in Ref. 1.

We note further that Joseph and Fosdick [5] predict, for the incompressible Newtonian fluid, corrections proportional to $\Omega^4$ due to finite values of $u_r$ and $u_z$ immediately below the free surface. It is difficult to compare this correction with that due to finite compressibility, since the latter depends on the ratio $(\partial\eta/\partial\rho)/(\partial p/\partial\rho)$ and Joseph and Fosdick have explicitly solved for the former only in the narrow gap limit $(b-a) \ll b$. However, it is reasonable to assume that they are typically comparable in magnitude.

We conclude that the flow profile for the Newtonian liquid in principle is altered by finite compressibility effects, but the changes are very small and would be very difficult to detect experimentally.

### 4.3. Artificial Weissenberg Effect

According to the solution for the "second-order fluid" due to Joseph and Fosdick [5], a Weissenberg effect can occur provided $P_{yy} - P_{xx}$ is positive and $P_{zz} - P_{xx}$ is also positive and larger than three-fourths of $(P_{yy} - P_{xx})$. In terms of generalized viscosities, the equivalent conditions are $\eta_- > 0$, $\eta_0 < 0$, and $|\eta_0| > \frac{1}{4}\eta_-$.

For the solution in Ref. 1, $\gamma(a) = 0.767$, and according to Eqs. (7) and (8), $\eta_- = 0.0245$ and $\eta_0 = 0.0476$. Evidently the presence of a positive $\eta_0$ guarantees that an enhanced depression, rather than a Weissenberg effect, will occur.

However, we can create an artificial Weissenberg effect merely by changing the sign of Eq. (8) while leaving all other rheological properties of the soft-sphere liquid unchanged. While this alteration seems to be somewhat contrived, the resulting rheological properties, at least qualitatively, will more closely resemble those of a typical polymeric non-Newtonian liquid, except that the shear dilatancy properties of real polymeric liquids are at present unknown.

The results of the numerical solution for $P_{zz}(r) - P_{zz}(b)$ are shown in Fig. 1. After the first iteration, in which we assume $\delta\rho = 0$, the solution of

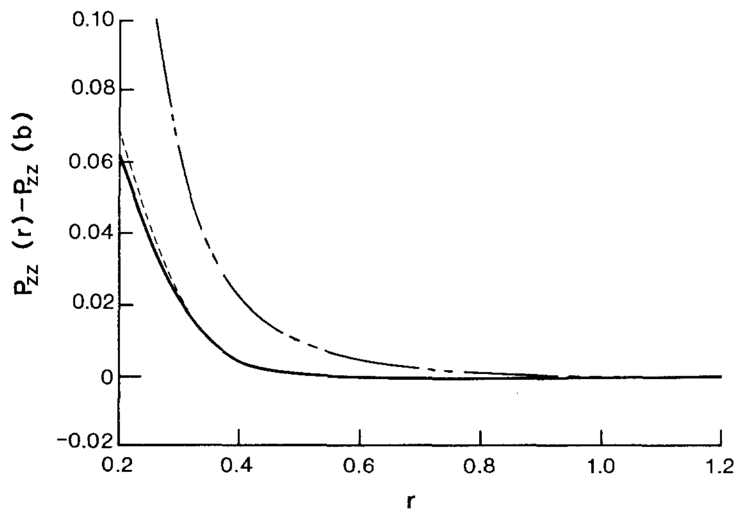


**Fig. 1.** Solutions for $P_{zz}(r) - P_{zz}(b)$, proportional to the free-surface height profile, for the replacement $\eta_0 \to -\eta_0$ from Eq. (13) for constant $\rho$ (dashed line), from Eq. (14) for constant $\rho$ (broken line), and the self-consistent solution of both equations with compressibility and variable density (solid line). The vertical axis intercept of the broken line, at 0.2528, is off the scale which has been chosen to resolve more clearly the dashed and solid lines.

**Table I.** Difference in Vertical Pressure Tensor Elements Between the Two Cylinders $[P_{zz}(a) - P_{zz}(b)]$

| $f$ | Eq. (13), constant $\rho$ | Eq. (14), constant $\rho$ | Self-consistent | $\delta\rho(a)$ |
|---|---|---|---|---|
| 1.0 | −0.0697 | 0.1588 | −0.0607 | −0.0205 |
| 0.5 | −0.0345 | 0.1823 | −0.0298 | −0.0196 |
| 0.0 | 0.0008 | 0.2058 | 0.0015 | −0.0187 |
| −0.5 | 0.0360 | 0.2293 | 0.0332 | −0.0177 |
| −1.0 | 0.0713 | 0.2528 | 0.0653 | −0.0168 |
| −1.5 | 0.1065 | 0.2762 | 0.0977 | −0.0158 |
| 1.0[a] | −0.0697 | −0.0470 | −0.0688 | −0.0019 |
| −1.0[a] | 0.0713 | 0.0470 | 0.0721 | 0.0021 |

[a] Shear dilatancy removed.

Eq. (13) yields $P_{zz}(a) - P_{zz}(b) = 0.0713$ and the solution of Eq. (14) yields $P_{zz}(a) - P_{zz}(b) = 0.2528$. The final, self-consistent solution yields $P_{zz}(a) - P_{zz}(b) = 0.0653$, or an 8.4% decrease from the initial solution of Eq. (13), which may be interpreted as a correction due to finite compressibility. This may be compared with the 12.9% decrease in the depth of the depression in the solution in Ref. 1 due to finite compressibility corrections.

We examine contributions of finite compressibility further by making the substitution $\eta_0 \to f\eta_0$ for a range of values of $f$ in the numerical algorithm. Results are listed in Table I for various multiples of $\eta_0$, where $f$ is the multiplicative factor and $\eta_0$ is a numerical result from the simulation in Ref. 2. The quantity $P_{zz}(a) - P_{zz}(b)$ is proportional to the height of the rod-climbing effect (positive) or the depth of depression (negative) as the case may be. The second column gives the solution in the incompressible limit and the fourth column gives the solution with compressibility.

A Weissenberg effect occurs for all negative values of $f$. The difference between the values in column 2 and those in column 4 is a measure of the contribution from finite compressibility and, in all cases, is at least of the order of 10%. We conclude that finite compressibility effects are likely to alter the free-surface profile of a fluid exhibiting a Weissenberg effect significantly, although not drastically.

## 4.4. Removal of Shear Dilatancy

The final case which we examine is a compressible non-Newtonian liquid without shear dilatancy. The rheological properties of the soft-sphere fluid are used, except that the coefficient of $\gamma^{3/2}$ in Eq. (5) and its density derivative are set equal to zero.

Results of the numerical calculation are shown in Fig. 2. The solution of Eqs. (10)–(13) for constant $\rho$ is, necessarily, identical to that in Ref. 1, i.e., $P_{zz}(a) - P_{zz}(b) = -0.0697$, but the constant-density solution of Eq. (14) gives $P_{zz}(a) - P_{zz}(b) = -0.0470$, in contrast to the value 0.1588 from Ref. 1. The self-consistent value is $-0.0688$, or a correction due to finite compressibility of only 1.3%. Furthermore, $\delta\rho$ is an order of magnitude smaller than the solution in the presence of shear dilatancy.

We also consider the case in which shear dilatancy is removed and, simultaneously, the sign of $\eta_0$ is reversed. Both results, denoted by footnote *a*, are presented in Table I; once again, the contributions due to finite compressibility are very small.

Our conclusion is that shear dilatancy and the sensitivity of the cylindrical flow problem to finite compressibility are closely related. An intuitive physical explanation is as follows: since $\gamma$ is large near $r = a$, the pressure must increase due to shear dilatancy. To counterbalance this increase so that the equations of motion are satisfied, the density must decrease near $r = a$. But since the normal pressure differences which give rise to an enhanced depression or Weissenberg effect are sensitive functions of density, the

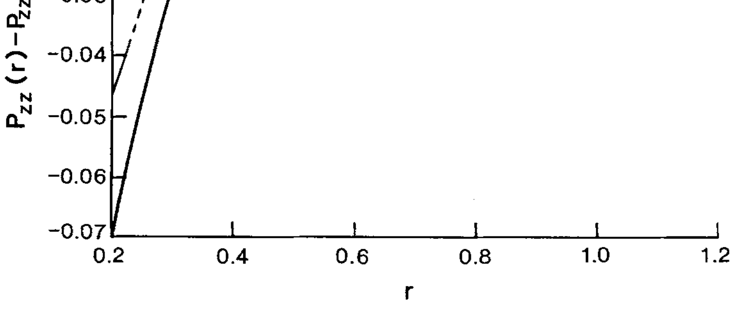


**Fig. 2.** Solutions for $P_{zz}(r) - P_{zz}(b)$ for the compressible liquid with shear dilatancy removed, from Eq. (13) for constant $\rho$ (solid line) and from Eq. (14) for constant $\rho$ (broken line). To within the resolution of the figure, the final self-consistent solution is indistinguishable from the solid line.

pressure and free-surface height profiles are significantly altered. In contrast, in the absence of shear dilatancy the changes due to finite compressibility are very small and their neglect may be justified.

## ACKNOWLEDGMENTS

The authors thank T. Paszkiewicz and Z. Petru of the University of Wroclaw, Poland, for assistance with early stages of this research and Karen Bowie for typing the paper. The work was supported by a grant from the Department of Energy, Office of Basic Energy Sciences.

## REFERENCES

1. J. C. Rainwater, H. J. M. Hanley, T. Paszkiewicz, and Z. Petru, *J. Chem. Phys.* **83**:339 (1985).
2. S. Hess and H. J. M. Hanley, *Int. J. Thermophys.* **4**:97 (1983).
3. R. B. Bird, R. C. Armstrong, and O. Hassager, *Dynamics of Polymeric Liquids, Vol. 1* (J. Wiley & Sons, New York, 1977).
4. K. Weissenberg, *Nature* **159**:310 (1947).
5. D. D. Joseph and R. L. Fosdick, *Arch. Rat. Mech. Anal.* **49**:321 (1973).
6. D. J. Evans and R. O. Watts, *Chem. Phys.* **48**:321 (1980).
7. S. Hess and H. J. M. Hanley, *Phys. Lett.* **98A**:35 (1983).